Results in Chemistry 5 (2023) 100846

Contents lists available at ScienceDirect

Results in Chemistry

journal homepage: www.sciencedirect.com/journal/results-in-chemistry

Synthesis, characterization, X-ray crystal structure, antioxidant, antimicrobial, and DNA binding interaction studies of novel copper (II)-isoxazole binary complexes

Marri Pradeep Kumar [a,b], Dasari Ayodhya [a], Aveli Rambabu [a,c], Shivaraj [a,*]

[a] Department of Chemistry, Osmania University, Hyderabad 500007, Telangana, India
[b] Department of Chemistry, Anurag University, Hyderabad 500088, Telangana, India
[c] Department of Science and Humanities, St Martin's Engineering College, Hyderabad 500100, Telangana, India

ARTICLE INFO

Keywords:
Isoxazole Schiff base
Cu(II) binary complex
Crystal structure
Antioxidant activity
Antimicrobial activity
DNA interaction

ABSTRACT

Cu (II) binary complexes of the type $[Cu(HL_x)_2]$, where x = 1–3, HL_1 = 2-((E)-(3,5-dimethylisoxazol-4-ylimino) methyl)-6-methylphenol (**C1**), HL_2 = 2-((E)-(3,5-dimethylisoxazol-4-ylimino)methyl)-6-ethoxyphenol (**C2**) and HL_3 = 2-((E)-(3,5-dimethylisoxazol-4-ylimino)methyl)-4,6-di-*tert*-butylphenol (**C3**) have been synthesized and characterized by various analytical, structural, and spectral methods. Single crystal X–ray diffraction analysis of ligand HL_1, complexes **C2** & **C3** revealed that the compounds are crystallized in monoclinic crystal system with the space groups of P1 21/c1 for HL_1 & **C2**, and P1 21/n1 for **C3**. The antioxidant studies of the synthesized Cu (II) complexes were carried out and it was shown as significant activity against DPPH radical. The synthesized Schiff bases and Cu(II) complexes were explored for antimicrobial activities and the complexes exhibited better potency against diverse microorganisms compared to Schiff bases as ligands. The interaction of Cu(II) complexes with CT–DNA has been explored with absorption and emission spectral techniques and the obtained results were evidence to the intercalative mode of DNA binding. The study of *Agarose gel electrophoresis* was resulted in three Cu(II) complexes stimulate the double strand breakage of pBR 322 plasmid DNA in the presence and absence of H_2O_2.

1. Introduction

Metal complexes with organic ligands as Schiff bases are being actively investigated as pharmacological agents, some of which have already found application in medical practice [1]. The Schiff bases are considered as "privileged ligands" due to their facile preparation, synthetic flexibility, and biocidal properties of the imine group [1]. Schiff bases obtained by the reaction of amines with salicylaldehydes has been often used as chelating ligands because they form stable complexes readily with most of the transition metals which have interesting structures, functional properties and potential applications in various areas such as catalysis, luminescent probes, analytical chemistry, magneto-structural chemistry, agrochemical and biological applications [2–4]. In general, based on the structure–property relationship, rational structural design, such as introducing different heterocyclic aryl groups, changing the electronic properties of the aryl units, was an important strategy in the high diversities in properties [5–6]. Isoxazole moiety, as one of a quite important five-membered heterocycle, contains nitrogen and oxygen atoms and they play a critical role to form complexes [7–8]. In addition, the complexes of transition metal ions with multi-dentate organic ligands have been the subject of intensive research because they not only have interesting spectral and magnetic properties, but they also possess a diverse spectrum of biological activities [9–10].

In recent years, many investigations associated with metal-based drugs show promising biological activity and are of great interest in chemistry and biology [11–12]. Therefore, the investigation of the factors, which impact the biological activity of metal complexes, makes feasible the design of metal complexes with specific medicinal, chemotherapeutic and pharmaceutical properties [13–14]. Many agile compounds using as drugs possess altered pharmacological and toxicological potentials when dispensed in the form of metal-based compounds [15]. Among transition metals, copper is present in enzymes in biological systems either alone or in combination with some other metal ions to discharge its role by redox reactivity, as well as its oxidative nature and

* Corresponding authors.
E-mail addresses: ayodhyadasari@gmail.com (D. Ayodhya), shivaraj_sunny@yahoo.co.in (Shivaraj).

https://doi.org/10.1016/j.rechem.2023.100846
Received 2 February 2023; Accepted 6 February 2023
Available online 9 February 2023

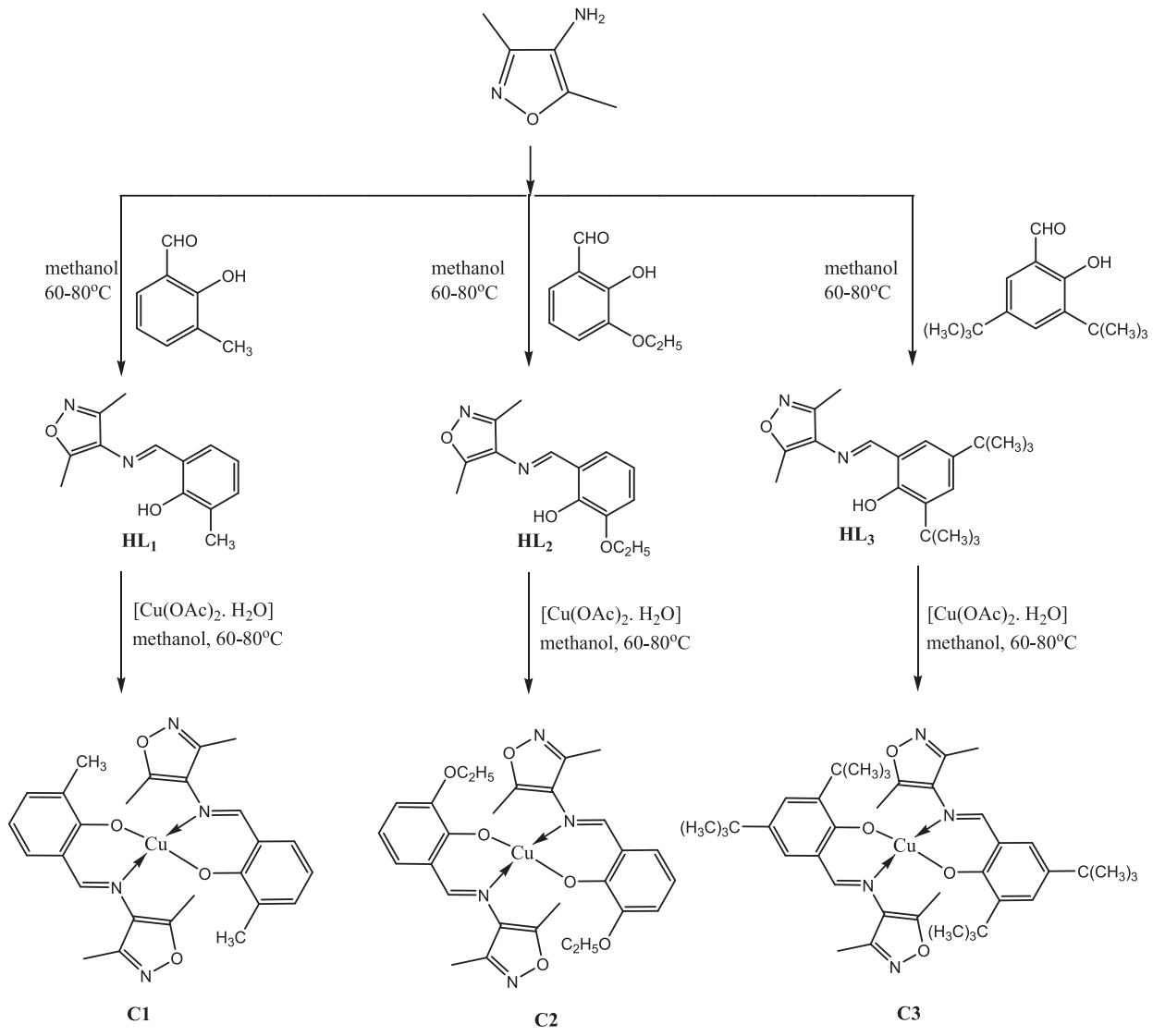

Scheme 1. Synthesis of isoxazole Schiff bases and their binary Cu(II) complexes.

bio-essential activity [16–18]. Copper is the third most abundant element in human body and it is present in many metallo-proteins and forms stable complexes with Schiff bases [19]. It accumulates in tumours due to the selective permeability of cancer cell membranes and is an efficient DNA cleaving agent. The copper complexes constitute an important class of molecules from several point of view viz. bio-inorganic, catalysis and magnetism.

Cu (II) complexes play a vital role in the active sites of a large number of metalloproteins in biological systems and potential application for many catalytic processes in living organisms that involve electron transfer reactions or activation of some antitumor substances. Indeed, copper (II) chelates have been found to interact with biological systems and to exhibit antineoplastic activity and antibacterial, antifungal, and anticancer activity [7–8]. In addition, it has been found that copper complexes interact non-covalently with the DNA double helix rather than creating coordinated covalent adducts [20]. The interaction of metal complexes with DNA has become the core subject of investigation for many researchers. DNA is generally the primary intracellular target of anticancer drugs, and their efficiency is exerted through the binding ability of these compounds to DNA. This is the core behind the design and discovery of new and more efficient drugs [21]. Copper synthetic compounds are able to promote nucleic acid (DNA) cleavage and are therefore worth investigating both in vitro and in vivo against cancer cells [22].

Isoxazole-metal complexes are often postulated as intermediates in reactions of considerable synthetic utility, for example the reductive ring opening of isoxazoles. Several isoxazole-metal complexes have been reported and well characterized. In a review of the literature of isoxazole-metal complexes [7–8], the binding characteristics of the isoxazoles in the complexes have been examined, and some tentative conclusions regarding the regularity of isoxazole complexation behavior have been discussed. Based on these aspects, it is important and interesting to study the interactions between Cu (II) and Schiff bases ligands derived from isoxazoles. In continuation with our interest in Schiff base ligands and their copper complexes with enhanced biocidal activities [23–24], the present work describes the synthesis of isoxazole Schiff base ligands (HL_1–HL_3) and their Cu(II) complexes (**C1**–**C3**). The new compounds have been characterized by elemental analysis, spectroscopic techniques, and single-crystal X-ray analysis. The synthesized compounds were investigated to estimate the antioxidant, antimicrobial, DNA binding & DNA cleavage (oxidative & photolytic) interaction properties.

2. Experimental

2.1. Materials

The chemicals, reagents, and solvents were purchased with AR grade. Purified solvents were used in the synthetic procedure of Schiff bases and metal complexes. Copper(II) acetate monohydrate [$Cu(OAc)_2{\cdot}H_2O$], 4-amino-3,5-dimethyl isoxazole amine, 2-hydroxy-3-methylbenzaldehyde, 3-ethoxy-2-hydroxybenzaldehyde and 3,5-di-*tert*-butyl-2-hydroxybenzaldehyde were purchased from Sigma-Aldrich chemicals, and used without further purification. Calf thymus and supercoiled plasmid pBR322 DNAs were purchased from Genei Laboratories Pvt Ltd, Bangalore, India and kept at 4 °C. Chemicals used for antimicrobial activity and DNA studies are obtained from Merck and Hi-Media Limited. Deionised double distilled water was used to prepare TAE buffer (40 mM Tris-acetate, 1 mM EDTA) solution at pH 7.2 for DNA binding and cleavage studies.

2.2. Instruments

The elemental composition and percentages of carbon, hydrogen and nitrogen of the compounds were estimated using Perkin Elmer 240C (USA) CHN analyzer. The high resolution X-ray diffraction data for compounds were collected on Bruker AXS (Kappa Apex 2) CCD diffractometer equipped with graphite monochromator Mo (Kα) (λ = 0.7107 Å) radiation source at 296(2) K. The FT-IR spectra of the Schiff bases and their Cu(II) complexes were recorded on a Perkin-Elmer Infrared model-337 spectrophotometer in the range 4000–400 cm^{-1} using KBr pellet method. UV–vis absorption spectra of the compounds were recorded on a Schimadzu UV–vis 2600 spectrophotometer in the region of 200–800 nm at room temperature. The magnetic moments of Cu(II) complexes were measured on Gouy balance model 7550 using the reference, $Hg[Co(SCN)_4]$. The melting points of all the compounds were determined using Polmon instrument (model No. MP-96). The ^1H & ^{13}C NMR spectra were recorded in $CDCl_3$ on BRUKER 400 MHz spectrometer using TMS as a reference at room temperature. ESI mass spectra were recorded on a VG AUTOSPEC mass spectrometer. The ESR spectra were recorded on a JES–FA200 ESR spectrometer (JEOL–Japan). Fluorescence emission spectra were collected with Hitachi F7000 spectrofluorometer using 1 cm path length cuvettes at 25 °C. Gel electrophoresis was executed on GeNei electrophoresis apparatus. The thermogravimetric analysis was carried out in an inert nitrogen atmosphere on Shimadzu TGA–50H thermal analyser with a heating rate of 10 °C min^{-1} in the temperature range of 30–1000 °C.

2.3. The synthesis of ligands and their Cu(II) complexes

2.3.1. Preparation of ligands HL_1 – HL_3

In the synthesis of ligands (HL_1 – HL_3), the 4-amino-3,5-dimethyl isoxazole amine (1.0 mmol) and 2-hydroxy-3-methylbenzaldehyde (1.0 mmol)/3-ethoxy-2-hydroxybenzaldehyde (1.0 mmol)/3,5-di-*tert*-butyl-2-hydroxybenzaldehyde (1.0 mmol) were refluxed in methanol solution at 60–70 °C with continuous stirring for 3 h (Scheme 1). After cooling to room temperature, the dark yellow coloured precipitate was filtered off and washed with cold methanol and petroleum ether in several times. Further recrystallized from methanol and dried in a vacuum desiccators over P_4O_{10}. The progress of reaction was monitored by TLC.

2.3.1.1. 2-((E)-(3,5-dimethylisoxazol-4-ylimino)methyl)-6-methylphenol (HL₁). Yield: 91 %. Anal. calc. for $C_{13}H_{14}N_2O_2$: C(%), 67.81; H(%), 6.13; N(%), 12.17. Found: C(%), 67.59; H(%), 6.32; N(%), 12.41. IR (KBr disks, cm^{-1}): $\upsilon_{(OH)}$ 3448, $\upsilon_{(CH=N)}$ 1608, $\upsilon_{(C—O)}$ 1208. UV–Visible (DMSO; λ^{max}, nm (cm^{-1})): 275 (36364), 307 (32573), 341 (29326). ^1H NMR (400 MHz, $CDCl_3$): δ12.97 (s, 1H), 8.57 (s, 1H), 7.27–7.24 (m, 1H), 7.19 (dd, J = 7.78, 1.26 Hz, 1H), 6.86 (t, J = 7.53 Hz, 1H), 2.50 (s, 3H), 2.40 (s, 3H), 2.31 (s, 3H). ^{13}C NMR (100 MHz, $CDCl_3$): δ = 163.4, 160.0, 159.0, 154.8, 134.3, 129.7, 126.3, 125.4, 118.8, 118.3, 15.4, 11.3, 10.8. Mass (*m/z*): 231 $[M + H]^+$ **(Fig. S1-S5).**

2.3.1.2. 2-((E)-(3,5-dimethylisoxazol-4-ylimino)methyl)-6-ethoxyphenol (HL₂). Yield: 93 %. Anal. calc. for $C_{14}H_{16}N_2O_3$: C(%), 64.60; H(%), 6.20; N(%), 10.76. Found: C(%), 64.31; H(%), 6.32; N(%), 10.49. IR (KBr disks, cm^{-1}): $\upsilon_{(OH)}$ 3442, $\upsilon_{(CH=N)}$ 1614, $\upsilon_{(C—O)}$ 1254. UV–Visible (DMSO; λ^{max}, nm (cm^{-1})): 280 (35714), 310 (32258), 353 (28329). ^1H NMR (400 MHz, $CDCl_3$): δ13.16 (s, 1H), 8.61 (s, 1H), 7.01–6.95 (m, 2H), 6.88 (t, J = 7.78 Hz, 1H), 4.15 (q, J = 21.08, 14.05, 7.03 Hz, 2H), 2.51 (s, 3H), 2.41 (s, 3H), 1.52 (t, J = 7.03 Hz, 3H). ^{13}C NMR (100 MHz, $CDCl_3$): δ162.8, 160.4, 154.7, 150.9, 147.7, 125.1, 123.4, 119.1, 118.8, 116.0, 64.5, 14.9, 11.3, 10.9. Mass (*m/z*): 259.05 $[M-H]^+$ **(Fig. S6-S10).**

2.3.1.3. 2-((E)-(3,5-dimethylisoxazol-4-ylimino)methyl)-4,6-di-tert-butylphenol (HL₃). Yield: 87 %. Anal. calc. for $C_{20}H_{28}N_2O_2$: C(%), 73.14; H (%), 8.59; N(%), 8.53. Found: C(%), 73.39; H(%), 8.41; N(%), 8.35. IR (KBr disks, cm^{-1}): $\upsilon_{(OH)}$ 3454, $\upsilon_{(CH=N)}$ 1611, $\upsilon_{(C—O)}$ 1202. UV–Visible (DMSO; λ^{max}, nm (cm^{-1})): 276 (36232), 300 (33333), 348 (28736). ^1H NMR (400 MHz, $CDCl_3$): δ13.13 (s, 1H), 8.58 (s, 1H), 7.46 (d, J = 2.51 Hz, 1H), 7.15 (d, J = 2.51 Hz, 1H), 2.51 (s, 3H), 2.41 (s, 3H), 1.47 (s, 9H), 1.33 (s, 9H). ^{13}C NMR (100 MHz, $CDCl_3$): δ164.9, 159.5, 157.9, 154.9, 140.8, 137.2, 128.3, 126.6, 125.7, 118.2, 35.1, 34.2, 31.5, 29.4, 11.3, 10.7. Mass (*m/z*): 327 $[M-H]^+$ **(Fig. S11-S15).**

2.3.2. Synthesis of binary Cu(II) complexes C1–C3 with HL_1-HL_3

The binary Cu(II) complexes **C1**–**C3** were synthesized by refluxing Cu(II) acetate mono hydrate (1.0 mmol) in methanol with corresponding bidentate Schiff bases HL_1–HL_3 (2.0 mmol) respectively in a round bottom flask (250 ml) equipped with magnetic stirrer for 3 h at the temperature range 60–70 °C. The dark brown coloured precipitates appeared on cooling were separated by filtration, washed with methanol and petroleum ether in several times and dried in a vacuum desiccators over P_4O_{10} (Scheme 1).

2.3.2.1. $[Cu(L_1)_2]$ (C1). Yield: 89 %. M.P: 183 °C. Mol Wt: 522. Anal. Calcd. for $CuC_{26}H_{26}N_4O_4$: C(%), 59.82; H(%), 5.02; N(%), 10.73. Found: C(%), 59.98; H(%), 5.13; N(%), 10.68. IR (KBr) (cm^{-1}): $\upsilon_{(C=N)}$ 1600, $\upsilon_{(C—O)}$ 1192, $\upsilon_{(Cu\text{-}O)}$ 563, $\upsilon_{(Cu\text{-}N)}$ 478. ESR: $g_{||}$=2.1864, $g_{\perp}$=2.0826, G = 1.9190. UV–vis (DMSO) λ^{max}/nm (cm^{-1}): 258 (38760), 284 (35211), 391 (25575), ε ($M^{-1}cm^{-1}$) (0.11×10^5). μ_{eff} (BM): 1.79. Mass (*m/z*): 560 $[M + K]^+$ **(Fig. S16, S19, S22, S25, and S27).**

2.3.2.2. $[Cu(L_2)_2]$ (C2). Yield: 87 %. M.P: 217 °C. Mol Wt: 582. Anal. Calcd. for $CuC_{28}H_{30}N_4O_6$: C(%), 57.77; H(%), 5.19; N(%), 9.62. Found: C(%), 57.84; H(%), 5.23; N(%), 9.55. IR (KBr) (cm^{-1}): $\upsilon_{(C=N)}$ 1602, $\upsilon_{(C—O)}$ 1194, $\upsilon_{(Cu\text{-}O)}$ 557, $\upsilon_{(Cu\text{-}N)}$ 487. ESR: $g_{||}$=2.1526, $g_{\perp}$=2.0607, G = 2.2191. UV–vis (DMSO) λ^{max}/nm (cm^{-1}): 279 (35842), 308 (32468), 361 (27701), ε ($M^{-1}cm^{-1}$) (0.12×10^5). μ_{eff} (BM): 1.89. Mass (*m/z*): 620 $[M + K]^+$ **(Fig. S17, S20, S23, 2, and S28).**

2.3.2.3. $[Cu(L_3)_2]$ (C3). Yield: 83 %. M.P: 221 °C. Mol Wt: 718. Anal. Calc. for $CuC_{40}H_{54}N_4O_4$: C(%), 66.87; H(%), 7.58; N(%), 7.80. Found: C (%), 66.59; H(%), 7.65; N(%), 7.91. IR (KBr) (cm^{-1}): $\upsilon_{(C=N)}$ 1587, $\upsilon_{(C—O)}$ 1172, $\upsilon_{(Cu\text{-}O)}$ 538, $\upsilon_{(Cu\text{-}N)}$ 488. ESR: $g_{||}$=2.1625, $g_{\perp}$=2.0655, G = 2.5348. UV–vis (DMSO) λ^{max}/nm (cm^{-1}): 258 (38760), 294 (34014), 414 (24155), ε ($M^{-1}cm^{-1}$) (0.15×10^5). μ_{eff} (BM): 1.83. Mass (*m/z*): 756 $[M + K]^+$ **(Fig. S18, S21, S24, S26, and S29).**

2.4. X–ray crystallography

Suitable single crystals of ligand HL_1, complexes **C2** & **C3** for X–ray structural determination were obtained by crystallization from

saturated solution of methanol, $CHCl_3$/DCM. Single crystals were mounted on Bruker AXS (Kappa Apex 2) CCD diffractometer equipped with graphite monochromator Mo (Kα) (λ = 0.7107 Å) radiation source [25]. A full sphere of data was collected with 100 % completeness for θ up to 25°. *ω* and *φ* scans were employed to obtain the data. The frame width for ω was set to 0.5 for data collection. The frames were integrated and data were reduced for Lorentz and polarization corrections were done using SAINT-NT [25]. The multi-scan absorption correction was applied to the data set. All structures were solved and refined using SHELXS-97 [26] and SHELXL-2014/7 [26], respectively. The non-hydrogen atoms were refined with anisotropic displacement parameter. The hydrogen atoms bonded to carbon atoms were fixed at chemically meaningful positions and were allowed to ride with the parent atom during refinement. Crystal **C3** molecule contains disordered solvent molecule which could not be modelled for a proper convergence was removed by using SQUEEZE program [27].

2.5. Antioxidant activity

The antioxidant activity of synthesized Cu(II) complexes was tested as individually at a final concentration of 0.3×10^{-6} to 3.0×10^{-6} M. The solution contained 1 ml of DPPH (diphenylpicrylhydrazyl radical, 5.0×10^{-5} M) and the given concentration range of the antioxidant solutions of complexes, resulting in a final concentration of DPPH solution is 3.0×10^{-5} M. The mixtures were vigorously mixed and allowed to stand in the dark for 30 min at 25 °C. The absorbance of the resulting solutions was measured at 517 nm against a blank sample containing only DPPH. The experiment was performed in triplicates along with ascorbic acid (IC_{50} = 4.8 mg/ml) as a positive control. The lower absorbance of the reaction mixture indicates higher free radical scavenging activity and the colour changes from violet to light yellow. The scavenging effect for •OH has been calculated from the below expression:

$$\text{Scavenging effect}(\%) = \left(\left(A_o - -A_{\text{sample}}\right)/A_o\right) \times 100$$

Where, A_o is the absorbance of the control and A_{sample} is the absorbance in the presence of the sample.

2.6. Antimicrobial assay

The *in-vitro* antimicrobial screening effects of the synthesized Schiff bases and their Cu(II) complexes were tested against the bacteria: *Escherichia coli (E. coli), Klebsiella pneumonia (K. pneumoniae), Pseudomonas putida (P. putida), Bacillus subtilis (B. subtilis)* and *Staphylococcus aureus (S. aureus)* and against the fungi: *Aspergillus niger (A. niger)* and *Candida albicans (C. albicans)* by the paper disc method using agar nutrient as the medium. In addition, standard drugs *Ampicillin* and *Ketoconazole* were also tested for their antibacterial and antifungal activity respectively, with the similar concentration conditions like test compounds. Copper acetate monohydrate salt ($[Cu(OAc)_2{\cdot}H_2O]$) used as a control test. The stock solution of the test compounds (100 μg/1 ml) was prepared by dissolving in DMSO. In experimental, a paper disc was kept on the agar medium inoculated with microorganisms. The disc was soaked with the test solution using a micropipette and the plate was incubated 24 h for bacteria and 48 h for fungi at 35 °C. During this period, the test solution was diffused and had shown its effect on the growth of the inoculated microorganisms.

2.7. DNA binding experiments

2.7.1. Preparation of stock solutions

The required concentration of CT–DNA stock solution was prepared by dissolving an appropriate amount of the original DNA (1 mg/mL) sample in 5 mM Tris–HCl/50 mM NaCl buffer of pH 7.2 at 25 °C. The DNA was found to be free of protein impurity from the ratio of the absorbance values of the CT-DNA at 260 and 280 nm in buffer solution as 1.9:1. Further the concentration of CT–DNA was ascertained by taking its molar absorption coefficient of 6600 M^{-1} cm^{-1} at 260 nm [28]. A stock solution of bromophenol blue was prepared by dissolving an appropriate sample in deionised double-distilled water. The solutions of the Cu(II) complexes were prepared by dissolving in DMSO solvent first to get a stock solution. All the prepared stock solutions were stored at 4 °C for complete dissolution and used over no more than 4 days.

2.7.2. UV–vis absorption titration study

Absorption titrations of all the synthesized Cu(II) complexes were recorded on Shimadzu UV–Vis 2600 spectrophotometer in the wavelength range 200–800 nm using 1 cm quartz micro–cuvettes. These electronic absorption titration experiments were accomplished with fixed complex concentration of 1.0×10^{-5} M, while varying the CT–DNA concentration from 0 to 1.0×10^{-5} M in 5 mM Tris–HCl/50 mM NaCl buffer solution of pH 7.2 at 25 °C. In each set of experiment, the self-absorption value of DNA was excluded. Spectral titrations were performed through the gradual addition of DNA solution to the quartz cuvette (1 cm path length) containing a working solution of the tested complexes. Absorbance spectra were recorded 10 min after each addition of DNA solution in order to allow incubation.

2.7.3. Fluorescence quenching study

The Fluorescence emission spectra of prepared Cu(II) complexes with CT–DNA were measured with Hitachi F7000 spectrofluorometer equipped with a Xenon lamp, at 25 °C in 5 mM Tris–HCl/50 mM NaCl buffer solution of pH 7.2. Solution containing CT–DNA and EB was titrated with varying concentrations of metal complexes. The concentrations of DNA and EB were maintained at 1.25×10^{-4} M and 1.25×10^{-5} M, respectively and the concentration of complexes were in the range of 0 to 6.0×10^{-5} M. While maintaining the fixed excitation wavelength at 350 nm, the emission spectra of DNA–EB with Cu(II) complexes were recorded in the wavelength range of 350–800 nm.

2.8. Nuclease activity assay

Gel electrophoresis is the well-known technique to inspect the DNA cleavage efficiency of the metal complexes. In the present investigation, agarose-gel electrophoresis method is used for both oxidative and photolytic cleavage of supercoiled pBR322 plasmid DNA with synthesized Cu(II) complexes in 5 mM Tris–HCl/50 mM NaCl buffer of pH 7.2. The cleavage activity over the DNA in the presence of H_2O_2 (oxidative cleavage) and UV light (photolytic cleavage) was conducted by dilution with the buffer to a total volume of 16 μL. Further the samples were incubated for 2 h at 37 °C and electrophoresis was performed at 50 V for 2 h in buffer solution using 1 % agarose gel contains 1.0 mg/mL ethidium bromide. The whole phenomenon of gel electrophoresis was monitored by a UV illuminator and the results were photographed by Gel Doc instrument.

3. Results and discussion

Schiff bases and their Cu(II) complexes were synthesized in a conventional manner, as shown in Scheme 1, and characterized by ^{1}H NMR, ^{13}C NMR, UV–Vis, FTIR, ESR, TGA, ESI mass spectrometry and single crystal X-ray diffraction studies. The spectral and elemental analysis data are in agreement with their chemical structures. The suitable single crystals of ligand HL_1, complexes ***C2*** and **C3** for X-ray diffraction were obtained on slow evaporation of the mixture of methanol, $CHCl_3$ or DCM solvents at room temperature. The complexes are in dark brown colour, non-hygroscopic, stable at room temperature and soluble in polar solvents such as DMF, DMSO, DCM and chloroform, slightly soluble in acetonitrile, ethanol and methanol, and insoluble in water. The elemental analysis shows that their composition is $[CuL_2]$, which was further confirmed by the single crystal analysis.

Table 1
Crystallographic data and structure refinement of ligand HL_1, complexes **C2** and **C3**.

Parameter	HL_1	**C2**	**C3**
Empirical formula	$C_{13}H_{14}N_2O_2$	$C_{28}H_{30}CuN_4O_6$	$C_{40}H_{54}CuN_4O_4$
Formula weight	230.26 g/mol	582.14 g/mol	718.42 g/mol
Temperature	296(2) K	296(2) K	296(2) K
Wavelength	0.71073 Å	0.71073 Å	0.71073 Å
Crystal size	0.130 × 0.220 × 0.250 mm	0.120 × 0.160 × 0.250 mm	0.100 × 0.220 × 0.250 mm
Crystal habit	clear light orange Block	clear dark brown Rectangular	metallic dark brown Rectangular
Crystal system	Monoclinic	monoclinic	Monoclinic
Space group	P 1 21/c 1	P 1 21/c 1	P 1 21/n 1
a	7.5577(4) Å	10.2941(2) Å	14.3984(3) Å
b	14.2887(8) Å	15.8903(4) Å	35.9686(9) Å
c	11.0257(5) Å	8.8863(2) Å	16.6284(4) Å
α	90°	90°	90°
β	98.700(3)°	108.2583(10)°	104.7070(10)°
γ	90°	90°	90°
Limiting indices	$-8\leq h\leq 8$, $-16\leq k\leq 15$, $-13\leq l\leq 13$	$-12\leq h\leq 12$, $-18\leq k\leq 18$, $-10\leq l\leq 10$	$-13\leq h\leq 16$, $-40\leq k\leq 40$, $-17\leq l\leq 18$
Volume	1176.96(11) $Å^3$	1380.41(5) $Å^3$	8329.5(3) $Å^3$
Z, Calculated density	4, 1.299 g/cm^3	4, 1.553 g/cm^3	4, 1.146 g/cm^3
Absorption coefficient	0.089 mm^{-1}	1.590 mm^{-1}	0.565 mm^{-1}
F(000)	488	664	3064
Measured reflections	7906	10,515	45,432
No. of independent reflections	2057 [R(int) = 0.0208]	2438 [R(int) = 0.0226]	12,480 [R(int) = 0.0530]
Coverage of independent reflections	99.8 %	100.0 %	99.6 %
Absorption correction	multi-scan	multi-scan	multi-scan
Max. and min. transmission	0.9880 and 0.9780	0.8320 and 0.6920	0.9460 and 0.8720
θ range for data collection	$\theta_{max} = 25.00°$, $\theta_{min} = 2.35°$	$\theta_{max} = 25.00°$, $\theta_{min} = 2.98°$	$\theta_{max} = 23.63°$, $\theta_{min} = 1.13°$
Final R indices [I greater than 2σ(I)]	R1 = 0.0524, w*R*2 = 0.1440	R1 = 0.0341, w*R*2 = 0.0954	R1 = 0.0577, w*R*2 = 0.1409
R indices (all data)	R1 = 0.0653, w*R*2 = 0.1566	R1 = 0.0427, w*R*2 = 0.1025	R1 = 0.0982, w*R*2 = 0.1557
Data/restraints/parameters	2057/0/162	2438/3/193	12,480/0/915
Structure Determination	SHELXL-2014/7 (Sheldrick, 2014)	SHELXL-2014/7 (Sheldrick, 2014)	SHELXL-2014/7 (Sheldrick, 2014)
Refinement method	Full-matrix least-squares on F^2	Full-matrix least-squares on F^2	Full-matrix least-squares on F^2
Function minimized	$\Sigma\, w(F_o^2 - F_c^2)^2$	$\Sigma\, w(F_o^2 - F_c^2)^2$	$\Sigma\, w(F_o^2 - F_c^2)^2$
Goodness-of-fit on F^2	1.068	1.054	1.039
Δ/σ_{max}	0.128	0.004	0.811
Weighting scheme	$w = 1/[\sigma^2(F_o^2)+(0.0657P)^2 + 0.7784P]$ where $P=(F_o^2 + 2F_c^2)/3$	$w = 1/[\sigma^2(F_o^2)+(0.0566P)^2 + 0.6938P]$ where $P=(F_o^2 + 2F_c^2)/3$	$w = 1/[\sigma^2(F_o^2)+(0.0776P)^2 + 1.5445P]$ where $P=(F_o^2 + 2F_c^2)/3$
Largest diff. peak and hole	0.279 and −0.271 e$Å^{-3}$	0.299 and −0.310 e$Å^{-3}$	0.511 and −0.346 e$Å^{-3}$
R.M.S. deviation from mean	0.042 e$Å^{-3}$	0.050 e$Å^{-3}$	0.053 e$Å^{-3}$
CCDC number	CCDC-2099025	CCDC-2099026	CCDC-2099027

3.1. X–ray diffraction studies

The obtained crystals of ligand HL_1 and complexes ***C2*** & **C3** were subjected to single crystal X–ray diffraction studies, then solved and refined. The detailed report of the structure refinement is shown in Table 1. In the unit cell, the HL_1 and complex ***C2*** crystallizes in the centro-symmetric monoclinic space group *P*21/*c*, with two equivalents and four equivalents, respectively, whereas the complex **C3** crystallizes in the centrosymmetric monoclinic space group *P*21/n with eight equivalents. The ORTEP diagram of crystals ligand HL_1, complexes ***C2*** & **C3** are shown in Fig. 1 drawn at 50 % ellipsoid probability. The Bond length between Cu atom and the coordinated nitrogen atom and the oxygen atom are 1.866 Å and 2.001 Å respectively. The mean plane deviation of the ring C1/*C*2/C3/C4/C5/C6 and the Cu atom is 0.313°. The interaction between molecules in the crystals ***C2*** & **C3** is mainly stabilized by C—H•••O and C—H•••N hydrogen bonding (Table 2). The bond length between the Cu atom and the coordinated nitrogen atom is in the range of 1.953–1.966 Å and for oxygen atom it is in the range of 1.886–1.895 Å. The crystal HL_1 which is a free ligand shows strong intra molecular hydrogen bonding with the nitrogen atom (O—H•••N hydrogen bonding, (Table 2).

3.2. FT − IR analysis

FT-IR analyses of the synthesized ligands $HL_1 - HL_3$ and their Cu(II) complexes **C1** − **C3** were carried out to identify and confirmation of the functional groups involved in the formation of Cu(II) complexes. The IR spectra of all the free ligands showed characteristic strong absorption bands in the range 1608–1614 cm^{-1}, attributed to the azomethine υ(HC = N) stretching vibrations, which were shifted to lower frequencies in the range 1587–1602 cm^{-1} in the Cu(II) complexes due to the chelation of the imine nitrogen to the Cu(II) ion [29]. The free ligands exhibit broad medium intensity bands in the range 3442–3454 cm^{-1} which are assigned to the phenolic υ(OH) stretching vibrations, upon complexation these bands disappear due to the oxygen atom coordinated with Cu (II) ion. The coordination of deprotonated phenolic moiety is also evidenced by the shift of υ(C—O) stretching bands of free ligands in the range 1202–1254 cm^{-1} to a lower frequency region 1152–1190 cm^{-1} in their complexes. The spectra of all Cu(II) complexes show that the characteristic bands observed in free ligands were shifted to lower frequencies, and concomitantly their intensities were also lowered. These results clear that the azomethine group was highly affected by complexation with Cu(II) ion. In addition, the bands in the range 538–563 and 478–488 cm^{-1} can be attributed to the υ(Cu − O) and υ(Cu − N) modes respectively [30].

3.3. Mass spectral analysis

The ligands and corresponding complexes were recorded by ESI-mass spectrometry and the peaks corresponding to the molecular ions were identified in the positive and/or negative mode, according to the calculated exact mass. The Schiff bases HL_1, HL_2 & HL_3 showed molecular ion peaks at *m/z* 231, 259 & 327 which attributed to the $[M + H]^+$, $[M-H]^+$ & $[M-H]^+$ fragments respectively. The Cu(II) complexes

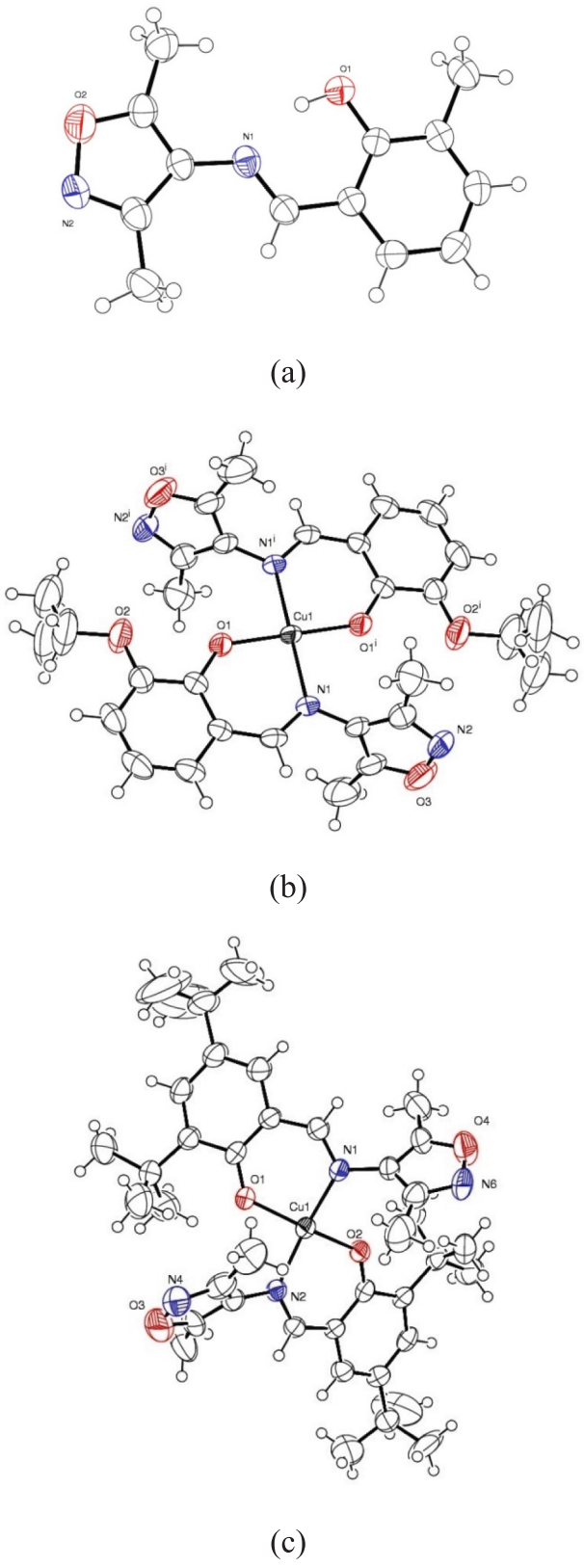

Fig. 1. Thermal ellipsoidal plots of (a) ligand HL_1, complexes (b) **C2** & (c) **C3** with atom labelling scheme. Displacement ellipsoids are drawn at 50% probability level except for the H atoms, which are shown as circles of arbitrary radius.(c).

Table 2
Hydrogen bonding in ligand HL_1, complexes **C2** and **C3**.

Compounds	H–bonds	Donor–H	Acceptor–H	Donor–Acceptor	Angle
HL_1	O1-H1O…N1	0.90(3)	1.74(3)	2.586(2)	155 (3)
C2	C14-H14C…O1	0.96	2.58	3.190(4)	121.6
	C12-H12A…N2	0.96	2.47	3.196(10)	132.8
	C7-H7…N2	0.93	2.61	3.540(3)	176.2
C3	C59-H59A…N4	0.96	2.63	3.303(6)	127.6
	C40-H40C…N11	0.96	2.69	3.408(7)	131.5
	C40-H40A…O7	0.96	2.58	3.499(6)	159.9

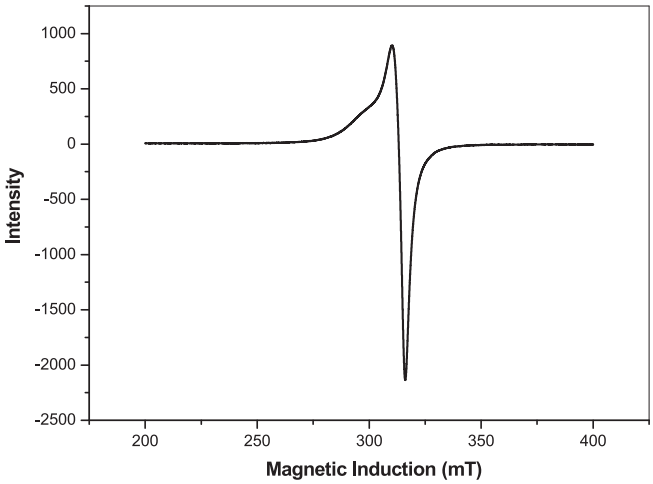

Fig. 2. ESR spectrum of Cu(II) complex (**C2**).

C1, ***C2*** & **C3** showed molecular ion peaks at *m/z* 560, 620 & 756 which ascribed to the $[M + K]^+$ ion peak and were thus the stoichiometry is in good agreement with the proposed structures of the mononuclear complexes.

3.4. ESR spectral studies

Electron spin resonance (ESR) spectroscopy is a significant tool in the analysis of the structures and environments of species that contain unpaired electrons. In the present investigation, the X band ESR spectra of complexes **C1**–**C3** were measured under liquid nitrogen temperature (77 K) in DMSO, see Fig. 2. The parameters $g_{||}$, $g_{\perp}$, and G values have been calculated and given in experimental section. From the observed experimental results, the trend follow the order as, $g_{||} > g_{\perp} > g_e(2.0023)$ suggesting the unpaired electron is localized in $dx^2–y^2$ orbital with $^2B_{1g}$ ground state [31]. Further all the Cu(II) complexes show that $g_{||}$ values are less than 2.3 ($g_{||}$less than2.3) suggesting the Cu–L bond is covalent in nature [32]. And the calculated 'G' values for complexes are in the range 1.91–2.53 which is lower than value of 4 suggesting that an exchange interaction is considerable according to Hathaway [33].

3.5. Thermal analysis

TGA technique has proved to be very useful in determining the loss

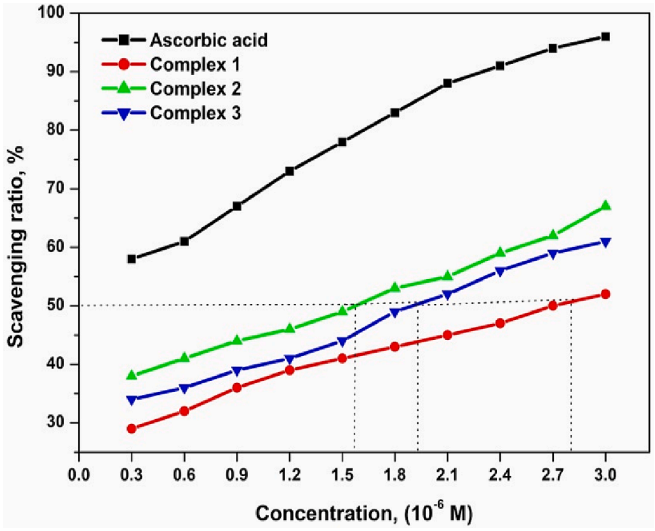

Fig. 3. The hydroxyl radical scavenging effect (%) of Cu(II) complexes (**C1** – **C3)** with the comparison of standard (ascorbic acid).

percentage of masses of the compounds and their thermal stability. The TGA curves of the synthesized Cu(II) complexes were recorded in the range of temperature 30 to 1000 °C with the heating rate is suitably controlled at 10 °C min^{-1} under nitrogen atmosphere. All thermograms clear that the thermal decomposition of all complexes **C1** – **C3** have a similar decomposition pattern included mainly in two steps. All Cu(II) complexes showed thermal stability up to 200 °C confirms the nonexistence of coordinated or lattice water molecules. The first step relates the loss of the part of ligand in the temperature range 225–375 °C, whereas the second step denotes the complete decomposition of complexes and the loss of their organic portion in the temperature range 415–785 °C, resulting copper oxide residue as final products.

3.6. Electronic spectra and magnetic measurements

The electronic spectra of free Schiff bases HL_1 – HL_3 and their complexes **C1** – **C3** were recorded in DMSO at room temperature using UV – Vis absorption spectrophotometer in the range of 200–800 nm and the corresponding data are given in experimental section. The low energy absorption bands of free Schiff bases appeared in the range of 341–353 nm are attributed to the azomethine chromophore $\pi \rightarrow \pi^*$ transitions. And the bands at higher energies 275–280 and 300–310 nm are associated with $\pi \rightarrow \pi^*$ transitions of aromatic benzene ring. These absorption bands were shifted to lower wavelengths with high energy region in their corresponding Cu(II) complexes. All Cu(II) complexes show an intense band in the range 361–414 nm is well in agreement with the allowed charge-transfer transitions. The usual feeble d–d transition band for the paramagnetic copper complexes cannot be noticed even at high concentrations. It may be lost in the low energy tail of the charge transfer transition [34,35]. The magnetic moments of all the complexes were also measured at room temperature and shown the magnetic moments in the range 1.79–1.89B.M, as expected for $3d^9$ paramagnetic Cu (II) complexes.

3.7. Hydroxyl radical scavenging activity

DPPH assay was carried out to determine the antioxidant capacity of the synthesized Cu(II) complexes. The complexes showed good antioxidant activity and depicted in Fig. 3. Such activity is due to the presence of OH group and efficient hydrogen donors that can stabilize the unpaired electrons, as a consequence, scavenge the free radicals. The results show that the ascorbic acid exhibits potential radical scavenging activity than the tested complexes at all concentrations. The IC_{50} value is the effective concentration at which 50 % of the DPPH radicals can be scavenged. A low IC_{50} value of a compound indicates ones high potentiality to act as a DPPH scavenger. Among these complexes, **C1** exhibits the maximum DPPH radical scavenging activity than the **C2** and **C3** (IC_{50} = 1.57, 1.96 and 2.81 μM, respectively), when compared to the ascorbic acid as standard.

3.8. Antimicrobial activity

The antimicrobial activity of Schiff bases HL_1 – HL_3 and their complexes **C1** – **C3** against various bacterial and fungal strains using the paper disc method was investigated and the diameter of the zone of inhibition (mm) around each disc is summarized in Table 3. It has been suggested that the ligands with the heteroatoms like N and O donor system might have inhibited enzyme production, since enzymes require a free hydroxyl group for their activity which could especially be susceptible to deactivation by the ions of the complexes. Upon coordination of free ligand to metal ion, the formed chelation reduces the polarity of the central metal ion to the maximum extent mainly because of the partial sharing of its positive charge with the available donor groups and possible π-electron delocalization within the whole cheated ring [36]. This chelation, in return, enhances the lipophilic character of the central atom which favours its penetration through the lipid layer of the membrane. However, the corresponding Cu(II) complexes exhibited efficient biological activity against tested microorganisms. Contrary to complexes, the free ligands and copper acetate salt exhibit slight inhibition towards all the microorganisms under the similar test conditions.

3.9. DNA binding

3.9.1. UV–vis absorption titration studies

To estimate the overall binding constants of the addition of increasing amounts of CT – DNA to the test sample of metal complexes is one of the most commonly used methods while noticing the changes in the absorption spectrum. To explore the possible binding mode and to

Table 3
Zone of inhibition results of Schiff bases and their Cu(II) complexes at 100 μg/mL concentration.

Compound	Bacteria(mm)						Fungi(mm)
	Gram-negative bacteria			Gram-positive bacteria		*A. niger*	*C. albicans*
	E. coli	*P. putida*	*K. pneumoniae*	*B. subtilis*	*S. aureus*		
HL_1	9.0 ± 0.2	9.0 ± 0.2	7.0 ± 0.2	9.0 ± 0.2	10.0 ± 0.1	10.0 ± 0.2	8.0 ± 0.2
HL_2	8.0 ± 0.1	7.0 ± 0.1	8.0 ± 0.1	7.0 ± 0.2	7.0 ± 0.2	11.0 ± 0.2	8.0 ± 0.2
HL_3	10.0 ± 0.1	8.0 ± 0.2	7.0 ± 0.2	8.0 ± 0.2	8.0 ± 0.2	9.0 ± 0.2	7.0 ± 0.2
C1	28.0 ± 0.2	22.0 ± 0.1	22.0 ± 0.1	24.0 ± 0.2	21.0 ± 0.2	24.0 ± 0.2	20.0 ± 0.1
C2	25.0 ± 0.2	19.0 ± 0.1	24.0 ± 0.2	20.0 ± 0.1	18.0 ± 0.2	21.0 ± 0.2	18.0 ± 0.2
C3	21.0 ± 0.2	20.0 ± 0.2	19.0 ± 0.2	18.0 ± 0.2	20.0 ± 0.1	22.0 ± 0.2	16.0 ± 0.1
$[Cu(OAc)_2{\cdot}H_2O]$	8.0 ± 0.1	7.0 ± 0.2	6.0 ± 0.1	6.0 ± 0.2	7.0 ± 0.2	10.0 ± 0.2	8.0 ± 0.2
Ampicillin	31.0 ± 0.2	30.0 ± 0.2	32.0 ± 0.1	31.0 ± 0.2	30.0 ± 0.1	–	–
Ketoconazole	–	–	–	–	–	33.0 ± 0.2	32.0 ± 0.2

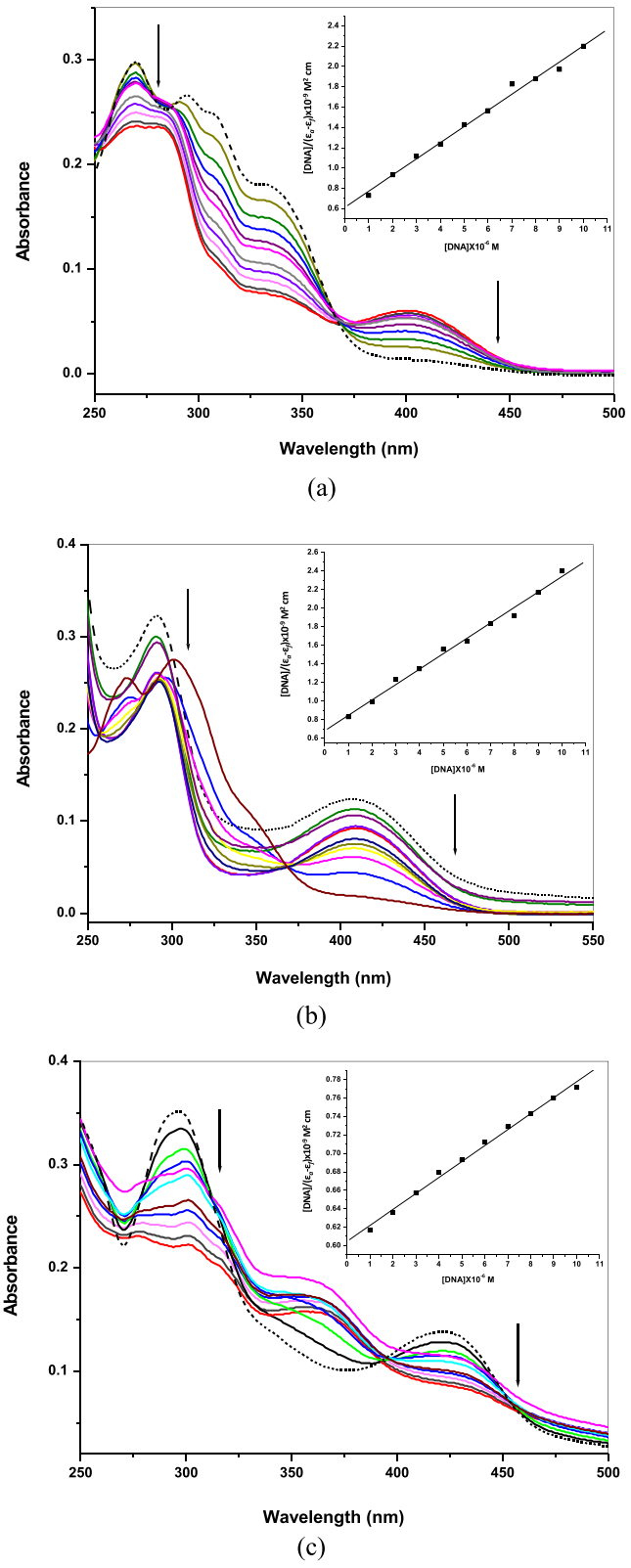

Fig. 4. Absorption spectra of C1 (a), C2 (b) and C3 (c) in the absence (·····) and presence (—) of ascending concentrations of CT − DNA in Tris-HCl buffer (pH 7.2). Conditions: [**complex**] = 1.0×10^{-5} M, [DNA] = $0 - 1.0 \times 10^{-5}$ M. Arrow (↓) shows the absorbance changes w.r.t. ascending concentrations of DNA. Inset: A linear plot for the calculation of binding constant, K_b.

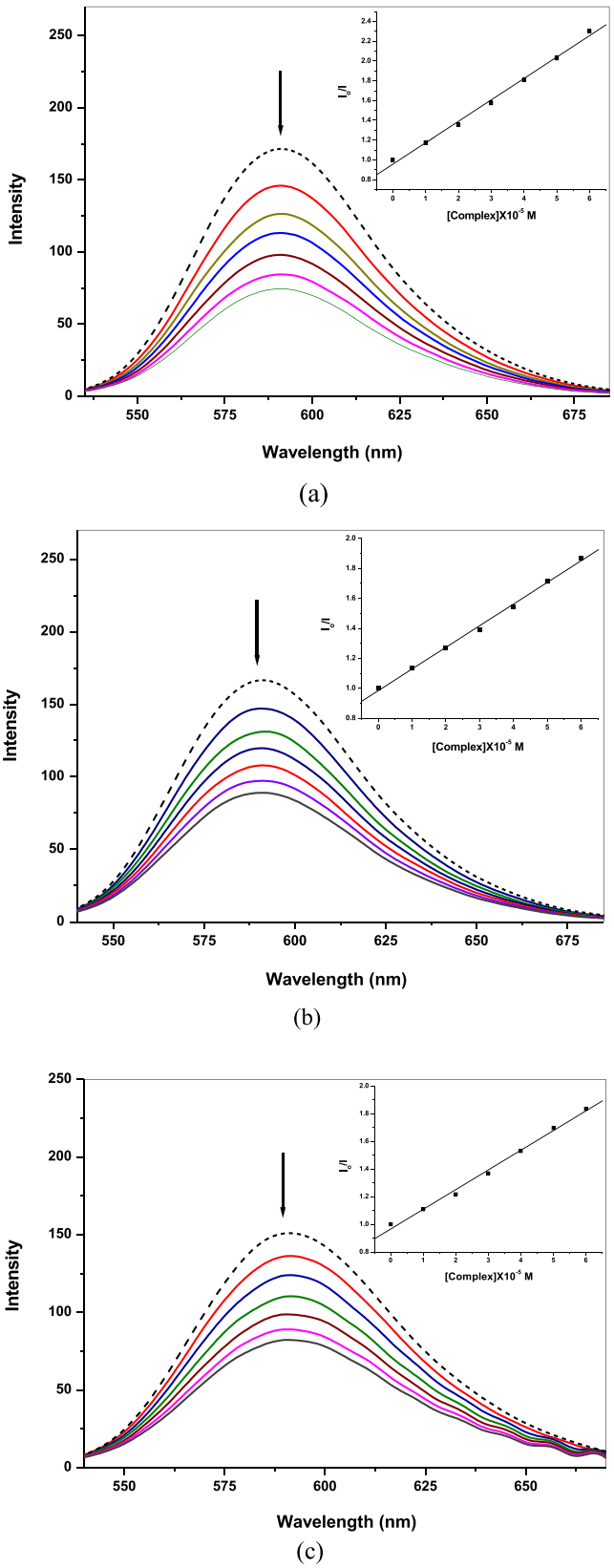

Fig. 5. Fluorescence quenching pictograms of **C1** (a), **C2** (b) and **C3** (c) against EB-DNA system: Arrow (↓) shows the emission intensity changes upon increasing concentration of the complexes. Inset: Stern-Volmer plots which shows quenching strength of complexes.

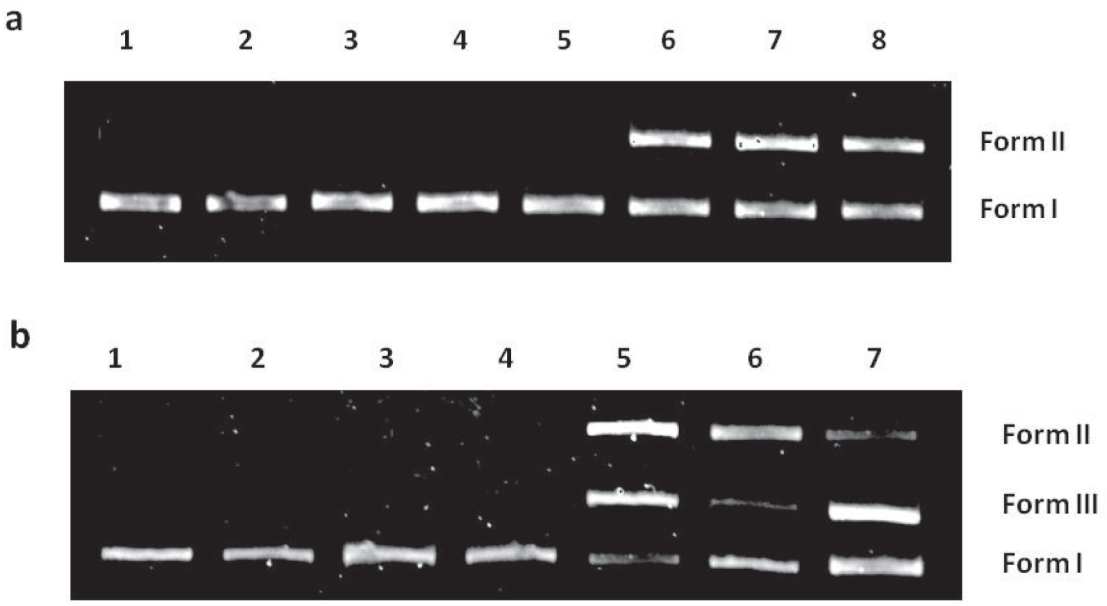

Fig. 6. A) Oxidative damage of pBR322 DNA (0.2 μg, 33.3 μM) at 37 °C in 5 μM Tris HCl/5 μM NaCl buffer by the ligands and their complexes. Lane 1: DNA control, Lane 2: DNA + H2O2 (1 μM): Lanes 3–5: DNA + H2O2 (1 μM) + $HL_1/HL_2/HL_3$ (20 μM), Lanes 6–8: DNA + H2O2 (1 μM) + complexes **C1/C2/C3** (20 μM). **b**) Photoactivated cleavage of pBR322 DNA (0.2 μg, 33.3 μM) at 37 °C in 5 μM Tris HCl/5 mM NaCl buffer by the ligands and their complexes, UV-light (long UV–365 nm). Lane 1: DNA control, Lanes 2–4: DNA + $HL_1/HL_2/HL_3$ (20 μM), Lanes 5–7: DNA + complexes **C1/C2/C3** (20 μM).

calculate the binding constant (K_b), the absorption titrations of investigated complexes were accomplished in the absence and presence of CT − DNA, illustrated in Fig. 4**.** The incremental addition of CT − DNA to Cu (II) complexes reveals significant hypochromism and slight red shift, which stipulates an intercalative mode of binding that involves a stacking interaction between the electronic state of the intercalating aromatic chromophore and that of the DNA base pairs [37]. The intercalation of complexes into the DNA base pairs associates with the π* orbital of the ligand chelated to metal can couple with π orbital of the base pairs of DNA, which leads to the degradation of π–π* transition energy. Besides this, the transition probabilities could be decreased by the coupling with π* orbital that is partially filled by electrons [38]. These spectral changes are consistent with the intercalation of complexes in to the DNA base stack. To compare the binding strength of Cu (II) complexes quantitatively, the intrinsic binding constants K_b of the complexes with CT − DNA were determined according to the following equation: $[DNA]/(\varepsilon_a-\varepsilon_f) = [DNA]/(\varepsilon_b-\varepsilon_f) + 1/K_b(\varepsilon_b-\varepsilon_f)$, where the apparent absorption coefficients ε_a, ε_f and ε_b correspond to A_{obs}/[complex], extinction coefficient for the free Cu(II) complex and for the complex in the fully bound form with DNA respectively and [DNA] is the concentration of CT − DNA in the base pairs [39]. Intrinsic binding constant (K_b) is the ratio of slope to intercept is calculated from the plot of $[DNA]/(\varepsilon_a-\varepsilon_f)$ versus [DNA]. Trend in potency of the binding association among the complexes against DNA follows the order: **C1** > **C2** > **C3** with the K_b values of $2.59 \pm 0.01 \times 10^5$, $2.43 \pm 0.02 \times 10^5$ and $2.96 \pm 0.01 \times 10^4$ M^{-1} respectively. The observed K_b values for Cu(II) complexes are less than that of typical classical intercalators like ethidium bromide (EB − DNA, $\sim 10^6$ M^{-1}) [40].

3.9.2. Fluorescence quenching study

Fluorescence quenching titrations of EB–DNA adduct were performed to further asses the mode of interaction of Cu(II) complexes towards DNA by the Ethidium bromide (EB) displacement method. The emission spectra of EB–DNA system in the absence and presence of Cu (II) complexes are presented in Fig. 5. The emission intensity of EB alone is very less which is dramatically increased when EB intercalates into DNA base pairs. The EB–DNA system shows a characteristic strong emission at 591 nm, when excited at 350 nm, indicating that the intercalated EB molecules have been successfully protected by neighbouring DNA base pairs from being quenched by H_2O. Such an enhancement in intensity of EB–DNA system can be quenched by other DNA binding agents such as metal complexes. The metal complexes compete with and replace the EB bound DNA by which a degradation in the emission intensity of EB–DNA takes place. Upon addition of complexes to EB–DNA system in an ascending manner, the emission intensity gradually decreases [41]. The inset plots, depicted in Fig. 5, having a straight line from the coordinates, 'I_0/I vs *[Q]*' shows the relative binding intensity of complexes towards DNA which is statistically determined by the classical Stern–Volmer equation [42]: $I_0/I = 1 + K_{sv}[Q]$. Here, I_0 and I are the fluorescence intensities in the absence and presence of complexes, respectively, K_{SV} is a linear Stern–Volmer quenching constant that is a measure of the quenching efficiency, which is dependent on the ratio of bound concentration of EB to the concentration of DNA and [Q] is the concentration of the quencher (complex). The K_{SV} values of Cu(II) complexes are calculated from the slope of I_0/I vs [Q] plot. From the above results the binding strength of the Cu(II) complexes with CT − DNA follow the order **C1** > **C2** > **C3** with the K_{SV} values of $1.48 \pm 0.02 \times 10^4$, $1.47 \pm 0.02 \times 10^4$ and $8.39 \pm 0.01 \times 10^3$ respectively, which is in consistent with UV − Vis absorption DNA binding results.

3.10. Nuclease activity

3.10.1. Oxidative cleavage

The oxidative damage of SC pBR 322 DNA along with Schiff bases HL_1 − HL_3 and their Cu(II) complexes **C1** − **C3** in the presence of hydrogen peroxide (H_2O_2) is executed and corresponding gel images are depicted in Fig. 6a**.** From the surveillance, lane 1 (control), lane 2 (DNA + H_2O_2) and lanes 3–5 (DNA + H_2O_2 + HL_1 − HL_3) didn't show any DNA cleavage whereas lanes 6–8 (DNA + H_2O_2 + **C1** − **C3**) did that means our prepared complexes are playing a catalytic role. Upon a strand cleavage, the supercoiled form is disrupted into the nicked circular (NC) form. An intensified contact of copper ions with H_2O_2 generates diffusible hydroxyl radical which is competent of damaging DNA

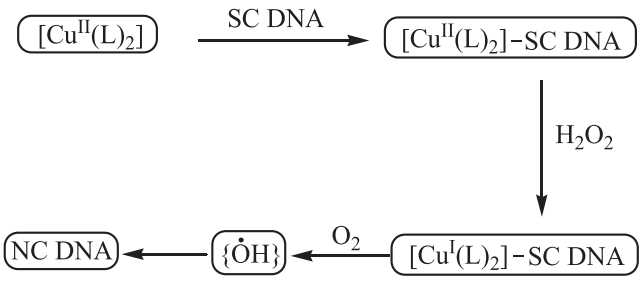

Scheme 2. A likely mechanism for an oxidative damage of DNA by Cu(II) complexes in the presence of H_2O_2.

by Fenton type or Haber–Weiss type chemistry, which escorts to exhibit superior cleavage potential towards plasmid DNA**.** As shown in Scheme 2**,** the complexes would initially intercalates into DNA base pairs to form a Cu(II)-DNA adduct, subsequently its reduction by the external agent H_2O_2 to form Cu(I)-DNA adduct, then produces hydroxyl radicals on reaction with oxygen. These hydroxyl radicals would then attack DNA to cause strand scission.

3.10.2. Photolytic cleavage

The capability of $HL_1 - HL_3$ and their complexes **C1** – **C3** to cleave SC pBR322 DNA is executed in the presence of UV light at irradiation of wavelength 345 nm and resultant gel images are illustrated in Fig. 6b**.** From the observation, lane 1 (control), 2–4 (DNA + $HL_1 - HL_3$) didn't show any DNA cleavage whereas lanes 5–7 (DNA + **C1** – **C3**) did show superior cleavage, due to the catalytic role of our synthesized complexes. Upon a strand cleavage, the supercoiled DNA is disordered into the nicked circular (NC) and linear forms. In this mechanism, singlet oxygen ($^1O_2$) plays a key role, which is accountable for cleavage of supercoiled plasmid pBR322 DNA.

4. Conclusion

In the present investigation, we have synthesized three Schiff bases $HL_1 - HL_3$ and their binary Cu(II) complexes **C1** – **C3** and characterized by several spectro-analytical techniques. The crystal structures of the Schiff base HL_1 and complexes **C1** & **C2** have been confirmed by the single crystal X-ray diffraction analysis. The characterized spectro-analytical techniques have been revealed that the structure of the all Cu(II) complexes is square planar. The DNA binding studies of the Cu(II) complexes examined by UV–vis absorption and fluorescence quenching titrations concluded that the binding mode of complexes against DNA is an intercalative manner. The order of binding affinity is found to be **C1** > **C2** > **C3**. Further supercoiled pBR322 DNA cleavage studies in the presence of H_2O_2 (oxidative cleavage) and UV light (photolytic cleavage) revealed that all the Cu(II) complexes prove a pronounced DNA cleavage activity. In addition, all the Cu(II) complexes showed promising antimicrobial activity than free Schiff bases due to the coordination effect.

CRediT authorship contribution statement

Marri Pradeep Kumar: Visualization, Investigation, Data curation, Writing – review & editing. **Dasari Ayodhya:** Visualization, Investigation, Data curation. **Aveli Rambabu:** Visualization, Investigation, Data curation, Writing – review & editing. **Shivaraj:** .

Declaration of Competing Interest

The authors declare that they have no known competing financial interests or personal relationships that could have appeared to influence the work reported in this paper.

Data availability

No data was used for the research described in the article.

Acknowledgements

Authors convey their heartfelt thanks to the Head, Department of Chemistry, Osmania University for provided that necessary research facilities. Authors are grateful to the Director, CFRD, OU & the SAIF, IIT Chennai for providing required spectral and analytical data. And authors are also extremely thankful to CSIR, DST – SERB and UGC – UPE (FAR), New Delhi for providing financial assistance.

Funding

No.

Appendix A. Supplementary data

CCDC 2099025, 2099026 and 2099027 contain the supplementary crystallographic data for ligand HL_1 complexes C**2** and **C3**, respectively. This data can be obtained free of charge via http://www.ccdc.cam.ac.uk/conts/retrieving.html, or from the Cambridge Crystallographic Data Centre, 12 Union Road, Cambridge CB2 1EZ, UK; fax: (+44) 1223-336-033; or e-mail: deposit@ccdc.cam.ac.uk. Supplementary data to this article can be found online at https://doi.org/10.1016/j.rechem.2023.100846.

References

[1] A. Frei, J. Zuegg, A.G. Elliott, M. Baker, S. Braese, C. Brown, F. Chen, C. G. Dowson, G. Dujardin, N. Jung, A.P. King, A.M. Mansour, M. Massi, J. Moat, H.A. Mohamed, A.K. Renfrew, P.J. Rutledge, P.J. Sadler, M.H. Todd, C.E. Willans, J.J. Wilson, M. A. Cooper, M.A.T. Blaskovich, Metal Complexes as a Promising Source for New Antibiotics, Chem. Sci. 11 (10) (2020) 2627–2639.
[2] S. Zehra, M.S. Khan, I. Ahmad, F. Arjmand, J. Biomol. Struct. Dyn. 37 (2019) 1863.
[3] X. Geng, Y. Zhang, S. Li, L. Liu, R. Yao, L. Liu, J. Gao, J. Mol. Struct. 1275 (2023), 134673.
[4] D. Ayodhya, Inorg. Chem. Commun. 148 (2023), 110295.
[5] N. Nishitani, T. Hirose, K. Matsuda, Chem. Commun. 55 (2019) 5099–5102.
[6] J.G. Huang, Y.F. Wang, L. Xu, Y.M. Liu, G.P. Zhou, J. Li, Z.R. Li, J. Phys. Org. Chem. e3973 (2019) 1–13.
[7] J.P. Rada, J. Forté, G. Gontard, V. Corce, M. Salmain, N.A. Rey, Chem. Bio. Chem. 21 (2020) 2474–2486.
[8] S. Sobhani, M. Pordel, S.A. Beyramabadi, J. Mol. Struct. 1175 (2019) 677–685.
[9] O.G. Shakirova, D.Y. Naumov, L.G. Lavrenova, S.K. Petkevich, V.I. Potkin, Inorg. Chem. Commun. 133 (2021), 108957.
[10] P. Kumar, M. Kapur, Organic Letters 22 (2020) 5855–5860.
[11] P. Krishnamoorthy, P. Sathyadevi, A.H. Cowley, R.R. Butorac, N. Dharmaraj, Eur. J. Med. Chem. 46 (2011) 3376.
[12] S. Ramakrishnan, D. Shakthipriya, E. Suresh, V.S. Periasamy, M.A. Akbarsha, M. Palaniandavar, Inorg. Chem. 50 (2011) 6458.
[13] P. Tyagi, M. Tyagi, S. Agrawal, S. Chandra, H. Ojha, M. Pathak, Spectrochim. Acta A 171 (2017) 246.
[14] W.A. Wani, S. Prashar, S.h. Shreaz, S. Gómez-Ruiz, Coord. Chem. Rev. 312 (2016) 67.
[15] A. Arbaoui, C. Redshaw, N.M. Sanchez-Ballester, M.R.J. Elsegood, D.L. Hughes, Inorg. Chim. Acta 365 (2011) 96.
[16] R. Loganathan, S. Ramakrishnan, E. Suresh, A. Riyasdeen, M.A. Akbarsha, M. Palaniandavar, Inorg. Chem. 51 (2012) 5512.
[17] S. Tabassum, S. Amir, F. Arjmand, C. Pettinari, F. Marchetti, N. Masciocchi, G. Lupidi, R. Pettinari, Eur. J. Med. Chem. 60 (2013) 216.
[18] V.M. Manikandamathavan, V. Rajapandian, A.J. Freddy, T. Weyhermuller, V. Subramanian, B.U. Nair, Eur. J. Med. Chem. 57 (2012) 449.
[19] M. Shabbir, Z. Akhter, I. Ahmad, S. Ahmed, V. McKee, H. Ismail, B. Mirza, Polyhedron 124 (2017) 117.
[20] C. Santini, M. Pellei, V. Gandin, M. Porchia, F. Tisato, C. Marzano, Chem. Rev. 114 (2014) 815.
[21] M. Fanelli, M. Formica, V. Fusi, L. Giorgi, M. Micheloni, P. Paoli, Coord. Chem. Rev. 310 (2016) 41.
[22] C.J. Lawrence, R.K. Dawe, K.R. Christie, D.W. Cleveland, S.C. Dawson, S.A. Endow, L. Wordeman, J. Cell Biol. 167 (2004) 19.
[23] M. Pradeep Kumar, S. Tejaswi, A. Rambabu, V.K.A. Kalalbandi, Shivaraj, Polyhedron 102 (2015) 111.
[24] M. Pradeep Kumar, N. Vamsikrishna, G. Ramesh, N.J.P. Subhashini, J.B. Nanubolu, Shivaraj, J. Coord. Chem. 70 (2017) 1368.
[25] Bruker, SADABS, Bruker AXS Inc., Madison, Wisconsin, USA (2012).

[26] G.M. Sheldrick, Acta Cryst. C71 (2015) 3.
[27] A.L. Spek, Acta Cryst. C71 (2015) 9.
[28] Z. Moradi, M. Khorasani-Motlagh, A.R. Rezvani, M. Noroozifar, J. Biomol. Struct. Dyn. 36 (2018) 779.
[29] M. AL-Noaimi, M.I. Choudhary, F.F. Awwadi, W.H. Talib, T.B. Hadda, S. Yousuf, A. Sawafta, I. Warad, Spectrochim. Acta A Mol. Biomol. Spectrosc. 127 (2014) 225.
[30] M. Hazra, T. Dolai, A. Pandey, S.K. Dey, A. Patra, J. Saudi Chem. Soc. 21 (2017) S240.
[31] A. Rambabu, S. Daravath, D. Shiva Shankar, Shivaraj, J. Mol. Struct. 1244 (2021) 131002.
[32] P.F. Rapheal, E. Manoj, M.R.P. Kurup, Polyhedron 26 (2007) 818.
[33] B.J. Hathaway, J. Chem, Soc., Dalton Trans (1972) 1196.
[34] C. Gokce, R. Gup, J. Photochem. Photobiol. B: Biol. 15 (2013) 122.
[35] S. Naskar, S. Biswas, D. Mishra, B. Adhikary, L.R. Falvello, T. Soler, Inorg. Chim. Acta 357 (2004) 4257.
[36] S. Rich, J.G. Horsfall, Phytopathology 42 (1952) 457.
[37] A. Rambabu, M. Pradeep Kumar, S. Tejaswi, N. Vamsikrishna, Shivaraj, J. Photochem. Photobiol. B: Biology 165 (2016) 147.
[38] T.R. Li, Z.Y. Yang, B.D. Wang, D.D. Qin, Eur. J. Med. Chem. 43 (2008) 1688.
[39] K. Sampath, S. Sathiyaraj, C. Jayabalakrishnan, Spectrochim. Acta A 105 (2013) 582.
[40] J.B. Lepecq, C. Paoletti, J. Mol. Biol. 27 (1967) 87.
[41] A. Rambabu, M. Pradeep Kumar, N. Ganji, S. Daravath, Shivaraj, J. Biomol. Struct. Dyn. 38 (2020) 307.
[42] K. Jeyalakshmi, Y. Arun, N.S.P. Bhuvanesh, P.T. Perumal, A. Sreekanth, R. Karvembu, Inorg. Chem. Front. 2 (2015) 780.